Available online at www.sciencedirect.com
SCIENCE DIRECT®
International Journal of Heat and Mass Transfer 47 (2004) 373–383
International Journal of HEAT and MASS TRANSFER
www.elsevier.com/locate/ijhmt

Direct identification of absorption and scattering coefficients and phase function of a porous medium by a Monte Carlo technique

M. Tancrez, J. Taine *

Laboratoire EM2C, École Centrale Paris—CNRS (UPR 288), 92295 Châtenay-Malabry Cedex, France

Received 27 January 2003; received in revised form 12 March 2003

Abstract

A general method of direct identification of absorption and scattering coefficients and phase function of porous media, assumed statistically homogeneous and isotropic, has been developed for wavelengths small in regard of the typical structure length (i.e. by neglecting diffraction). This method is here limited to a transparent fluid phase and an opaque solid phase. Diffuse and specular reflection laws and combination of these laws are considered. First results have been obtained for sets of Dispersed radius Overlapping Opaque Spheres (DOOS) in a transparent fluid phase, or sets of Dispersed radius Overlapping Transparent Spheres (DOTS) in an opaque solid phase. In the case of DOOS models, the absorption and scattering coefficients have the same analytical expressions as those characterizing the optically thin limit for any porous medium. For DOTS models, these coefficients have been, for porosity higher than 0.65, identified from Monte Carlo calculations versus the porosity or the specific area per unit volume of the fluid phase. For DOOS models, the phase functions have been expressed by a simple analytical expression in the case of a specular reflection law, and derived from Monte Carlo calculations in the case of the diffuse reflection law. For DOTS models, phase function have been numerically calculated from Monte Carlo calculations. The case of the combination of the two reflection laws is finally discussed.

1. Introduction

At high temperature, radiative transfer has to be accurately taken into account in many applications involving porous media of various types, such as fluidized and packed beds, catalytic reactors and fibers or foams in spatial thermal shields, etc. In the particular case of combustion within a porous medium, it has been emphasized [1] that radiative transfer inside the porous medium plays a prominent role in the flame stabilization and that scattering effects cannot be neglected. Prediction and optimization of the performances of such systems require that the radiative properties of the medium are characterized. Unfortunately, there is often a lack of such data.

The modeling of radiative transfer at a local scale in a porous structure with an opaque solid phase and a transparent fluid phase, taking into account absorption and reflection phenomena, is generally unaffordable for two reasons: (i) the medium structure is often only statistically known; (ii) huge calculation times and storage capacities would be required. On the other hand, a porous medium can, under some validity conditions, be treated as a continuous homogeneous absorbing and scattering medium. If the homogenization procedure is valid, the radiative properties of this equivalent medium have to be determined.

Many methods of characterization of radiative properties of porous media, considered as semi-transparent media, have been developed and a survey can be found in [2]. Some authors [3–6] have predicted the radiative properties of porous media from the geometric optics approximation and taken into account a small

* Corresponding author.

0017-9310/$ - see front matter © 2003 Elsevier Ltd. All rights reserved.
doi:10.1016/S0017-9310(03)00146-7

corrective term associated with diffraction. In the last reference, some parameters are also identified by using reflectance and transmittance measurements. Many studies are mainly based on these parameter identification methods or on inverse techniques. For a randomly packed bed of identical opaque spheres, equivalent absorption and scattering coefficients and parameters of a phase function of an arbitrary chosen type have been identified from experimental data of hemispherical transmittances and reflectances by using a least square fit approach and a discrete ordinate radiative transfer model [7]. Similar studies have been carried out for ceramics [8] or polyurethane foam [9]. An advantage of such a method is to be directly applied to an actual porous medium. Drawbacks are that radiative inverse problems are often ill-conditioned and the practical inversion requires to impose a particular type of phase function (isotropic, Henyey–Greenstein...) and an ETR resolution method.

Some authors have used a Monte Carlo approach to calculate transmittances, reflectances or intensities in porous media, at a local scale. By identifying these results with corresponding results obtained from a radiative transfer model applied to an equivalent semi-transparent medium, they have deduced values of extinction coefficient β, absorption coefficient κ and scattering coefficient σ, possibly depending on frequency. In a reference work [10], κ and σ have been identified by comparison with a two flux model for a randomly packed bed of non-overlapping identical spheres. Another study [11] has been carried out on the same bases for the same system. A three-dimensional calculation of the transmittance has been done, by a Monte Carlo method, for a finite bed of the same type [12]. A similar study [13], dedicated to fibrous media, deals with the calculation by a Monte Carlo method of the emittance of a set of semi-infinite cylinders. A Monte Carlo method has also been used in the determination, in an inverse problem, of both the albedo and the asymmetry parameter g of a medium of known extinction coefficient [14]. Other authors have shown that the Monte Carlo approach is practically the only way for taking into account shadow effects for a set of spheres, but do not modelize the coherence effects associated with dependent scattering [15–17]. In the last reference, a model of local coupling between radiation and conduction is proposed, but is limited to locally optically thick media. The Monte Carlo method gives a great amount of information on radiative transfer within the medium and enables to define a criterion for the homogenization availability. On the other hand, this method requires a precise knowledge of the porous morphology and of radiative properties of both the solid and fluid phases. The Monte Carlo method provides also a good understanding of the physics of radiative transfer which could ameliorate experimental methods.

The present paper deals with the modeling of a real porous medium as a continuous equivalent absorbing and scattering medium, characterized by a non-isotropic phase function. The medium morphology is assumed perfectly known and statistically isotropic and homogeneous. In principle, this morphology can be determined by experimental techniques. We assume that the fluid phase of the porous medium is transparent, and the solid phase is opaque, of known radiative properties at the local scale. Furthermore, we consider that the typical pore scale is much larger than the considered wavelength. This hypothesis is independent of the wavelength range. Consequently, we assume that the geometrical optics laws are valid in the medium at the local scale and that no diffraction effect occurs. In the same manner, we do not take into account polarization effects. In conclusion, scattering is here, at the continuous medium scale, a modeling of the reflection phenomena.

In the chosen local treatment of the medium, the extinction, absorption and scattering probabilities are calculated from a Monte Carlo technique. As far as the extinction, absorption and scattering coefficients can be defined, these coefficients are obtained by a direct identification of the previous probabilities with the corresponding expressions of the continuous medium approach. One originality of this work is to identify the previous quantities, directly from their definitions, without using a radiative transfer model based on the radiative transfer equation as commonly done [10,11], etc. When a scattering coefficient is defined, the corresponding phase function is simply deduced, from the application of the reflection laws to the medium in the local approach. This direct obtention of the phase function is also original. Section 2 deals with this general identification method for actual porous media.

Section 3 is an application of the method to a porous medium modeled either by a set of overlapping spheres of fluid, of centers randomly distributed in the solid phase or, on the contrary, of overlapping solid spheres, of centers randomly distributed in the fluid phase, which is another originality of this work. Both the radius and center location distributions could be adjusted from experimental results. Many actual porous media can be modeled by sets of spheres, in particular when they have been manufactured from spherical material elements, which have been removed at high temperature. For instance, catalytic burners made of cordierite are of the first previously defined type. Results related to the extinction, scattering and absorption coefficients are given and discussed in Section 3.

Results related to the scattering phase function are given and discussed in Section 4. The implementation of the data in radiative transfer applications is discussed in Section 5.

2. General identification method

This section deals with the principles of a general identification method, which can be applied to statistically homogeneous and isotropic porous media, characterized by an opaque solid phase and a transparent fluid phase, as long as the identification with an equivalent semi-transparent medium can be carried out.

2.1. Extinction and absorption coefficients

An originality of the present method is to identify the absorption and scattering coefficients and the phase function, directly from their physical definitions. This purpose is shown in Fig. 1a and b, which deal with the porous medium local approach and the continuous medium approach, respectively. As the porous medium is assumed statistically isotropic, we consider only an incident ray in an arbitrary given direction. In this actual medium, the elementary extinction, absorption and scattering phenomena affect any ray, in the given direction, issued from any point of the fluid phase of the plane cross-section $s = 0$ of Fig. 1a. As long as the porous medium is statistically homogeneous, the choice of a current point of the fluid phase in the the cross-section plane $s = 0$ is equivalent to the choice of a current point in all the volume of the fluid phase. This last approach will be here followed.

As the fluid is transparent, extinction occurs when a ray issued from a point M of the fluid phase hits a solid phase wall element I (see Fig. 2). This phenomenon only depends on the porous medium geometry and does not depend on radiation frequency. In the case considered here of an opaque solid, the ray is partially absorbed and partially reflected. From a physical point of view, the extinction of any ray is total at each point I. Indeed, the possible reflected ray corresponds to the propagation of radiation in another direction. The associated multiple scattering effect could be taken into account by the use of the radiative transfer equation, which is not the topic of the present paper.

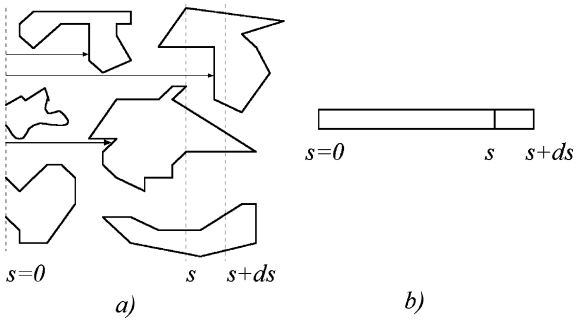

Fig. 1. (a) Schematic cross-section of an actual porous medium; (b) equivalent continuous semi-transparent medium.

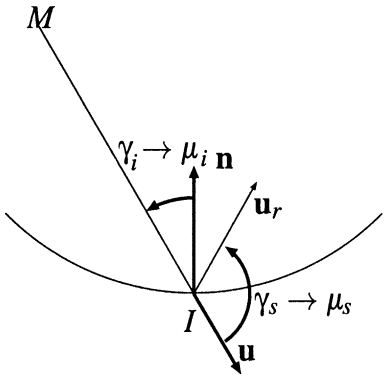

Fig. 2. Definition of the angles at the local scale.

In the Monte Carlo model, applied at the local scale, a current ray starts, as previously justified, from any random point $M(\mathbf{r})$ of the fluid phase. Total extinction (absorption and reflection) only occurs at the point I, which is the intersection of the ray with the interface. The extinction cumulated distribution function $G_e(s)$ is then equal, in this local model, to the cumulated distribution function of the length MI. This function only depends on the geometrical structure of the medium. In practice, it is defined by

$$G_e(s) = \int_0^s F_e(s')\,ds' = \frac{1}{V_F}\frac{1}{4\pi}\int_0^s \int_{V_F}\int_{4\pi} \delta[s' - s_0(\mathbf{r},\mathbf{u})] \times d\Omega(\mathbf{u})\,d\mathbf{r}\,ds', \quad (1)$$

where s is the abscissa from point M along the current ray, $F_e(s')$ the extinction distribution function, V_F the fluid phase volume, $d\Omega(\mathbf{u})$ the elementary solid angle associated with the current unit vector $\mathbf{u}$ of the ray MI, δ the Dirac δ function and $s_0(\mathbf{r},\mathbf{u})$ the length $|MI|$.

In the continuous medium approach, the extinction is characterized by an extinction coefficient β. The extinction distribution function f_e and the extinction cumulated distribution function g_e are defined by

$$f_e(s) = \beta \exp(-\beta s), \quad (2)$$

$$g_e(s) = 1 - \exp(-\beta s). \quad (3)$$

β is determined by identification of $G_e(s)$ and $g_e(s)$ by a least square fit method. The validity range of this identification can be deduced from the standard deviation associated with this method.

In the local model, the probability of absorption in the range $[s, s + ds]$ is

$$dP_a(s) = F_a(s)\,ds = \frac{1}{V_F}\frac{1}{4\pi}\int_{V_F}\int_{4\pi} \alpha'_v\{\gamma_i[\mathbf{n}(\mathbf{r},\mathbf{u}),\mathbf{u}]\} \times \delta[s - s_0(\mathbf{r},\mathbf{u})]\,d\Omega(\mathbf{u})\,d\mathbf{r}\,ds, \quad (4)$$

where $\alpha'_v(\gamma_i)$ is the directional absorption coefficient of the opaque interface, which depends on γ_i, angle between $-\mathbf{u}$ and $\mathbf{n}$ the local normal unit vector towards the fluid phase at point I (Fig. 2).

The corresponding probability of absorption for the homogenized continuous medium model, $dp_a(s)$ is defined as

$$dp_a(s) = f_a(s)\,ds = \exp(-\beta s)\kappa_v\,ds, \tag{5}$$

where κ_v is the continuous medium absorption coefficient. As β has been previously obtained, κ_v can be determined by identifying $G_a(s)$, calculated by the Monte Carlo method, i.e.

$$G_a(s) = \int_0^s F_a(s')\,ds', \tag{6}$$

with the corresponding function in the continuous medium approach, i.e.

$$\int_0^s f_a(s')\,ds' = [1 - \exp(-\beta s)]\kappa_v/\beta. \tag{7}$$

Let us notice that, in the particular case in which the incidence cosine

$$\mu_i = -\mathbf{n}\cdot\mathbf{u} = \cos\gamma_i \tag{8}$$

is statistically independent of the other parameters characterizing a current ray, in particular of $s_0(\mathbf{r},\mathbf{u})$, Eq. (4) simplifies as follows, by considering that the averaged value of the product of two statistically independent quantities is equal to the product of the averaged quantities, i.e.

$$F_a(s)\,ds = F_e(s)\,ds \int_0^1 \alpha'_v(\mu_i)F_i(\mu_i)\,d\mu_i, \tag{9}$$

where $F_i(\mu_i)$ is the distribution function of μ_i.

On the other hand, let us notice that, if α_v is independent of γ_i (case of the diffuse reflection law), we simply obtain

$$F_a(s) = \alpha_{v\mathrm{diff}}F_e(s), \tag{10}$$

which leads to

$$\kappa_{v\mathrm{diff}} = \beta\alpha_{v\mathrm{diff}}. \tag{11}$$

2.2. Optically thin medium asymptotic case

In the asymptotic case of an optically thin, statistically isotropic and homogeneous porous medium, both the extinction coefficient β and the absorption coefficient κ_v have simple expressions, whatever are the reflection law of the interface and the morphology of the porous medium. These expressions will be used in the following as references.

As, in these conditions, no self-absorption phenomenon occurs, the flux emitted by an elementary fluid volume dV_F in the local model can be identified with the same flux expressed in the continuous medium approach, i.e.

$$\pi\alpha_v^h I_v^\circ(T)\,dS = 4\pi\kappa_v I_v^\circ(T)\,dV_F, \tag{12}$$

where dS is the interface area in the element dV_F, $I_v^\circ(T)$ the equilibrium intensity and α_v^h the hemispherical absorptivity of the interface, given by

$$\alpha_v^h = \pi^{-1}\int_{2\pi}\alpha'_v(\gamma_i)\cos(\gamma_i)\,d\Omega. \tag{13}$$

Finally, at the optically thin limit, κ_v is given by

$$\kappa_v = (\mathscr{A}/4)\alpha_v^h, \tag{14}$$

where $\mathscr{A}$ is the specific interface area per unit volume of fluid phase.

The extinction coefficient can also be simply expressed at the optically thin limit. As the medium has been assumed statistically isotropic, we only consider one incident direction $\mathbf{u}$ normal to an arbitrary cross-section $\mathscr{S}$ of the fluid phase. $\beta\,ds$ is the probability that any ray issued from a point M of $\mathscr{S}$ in the direction $\mathbf{u}$, reaches the interface at a point $I(\mathbf{R})$ such as MI is less than ds, i.e.

$$\beta\,ds = \lim_{\mathscr{S}\to\infty}\left[\int_{d\Sigma} -\mathbf{n}(\mathbf{R})\cdot\mathbf{u}\,d\mathbf{R}/\mathscr{S}\right]. \tag{15}$$

In Eq. (15), $d\Sigma$ is the fraction of the interface area in the volume $\mathscr{S}\,ds$ viewed in the direction $\mathbf{u}$, which is equal, as the interface is randomly oriented, to $\mathscr{S}\,ds\,\mathscr{A}/2$ (only half of the area is viewed in the direction $\mathbf{u}$). For the same reason, Eq. (15) becomes

$$\beta = \mathscr{A}\int_0^{\pi/2}\frac{2\pi\sin(\gamma_i)}{4\pi}\cos(\gamma_i)\,d\gamma_i = \mathscr{A}/4, \tag{16}$$

which represents the asymptotic expression of β for a statistically isotropic and homogeneous porous medium at the optically thin limit.

2.3. Phase function

In as much as the scattering coefficient has been defined, the scattering phase function $p_v(\mathbf{u},\mathbf{u}_r)$ is the distribution function associated with the probability that, in the spherical frame of axis $\mathbf{u}$, the reflected ray belongs to a given elementary solid angle $d\Omega_r(\mathbf{u}_r)$, i.e.

$$p_v(\mathbf{u},\mathbf{u}_r)\,d\Omega_r(\mathbf{u}_r) = \frac{\int_{V_F}\rho''_v[\mathbf{u},\mathbf{u}_r,\mathbf{n}(\mathbf{u},\mathbf{r})]\mathbf{u}\cdot\mathbf{n}(\mathbf{u},\mathbf{r})\,d\mathbf{r}\,d\Omega_r(\mathbf{u}_r)}{\int_{4\pi}\int_{V_F}\rho''_v[\mathbf{u},\mathbf{u}'_r,\mathbf{n}(\mathbf{u},\mathbf{r})]\mathbf{u}\cdot\mathbf{n}(\mathbf{u},\mathbf{r})\,d\mathbf{r}\,d\Omega_r(\mathbf{u}'_r)}, \tag{17}$$

where $\rho''_v(\mathbf{u},\mathbf{u}_r,\mathbf{n})$ is the bi-directional reflectivity in the spherical frame of axis $\mathbf{n}$, as defined in [18]. In Eq. (17), ρ''_v is taken equal to zero if $\mathbf{u}_r$ is towards the solid phase.

As a consequence of the statistical isotropy of the porous medium, the scattering phase function is independent of the incident direction and, more restrictively, assumed only dependent on the cosine μ_s of the scattering angle between the incident and reflected rays, i.e.

$$\mu_s = \mathbf{u}\cdot\mathbf{u}_r. \tag{18}$$

Under this assumption, p_v becomes

$$p_v(\mu_s) = \frac{\int_{V_F}\int_{4\pi}\int_{4\pi}\delta(\mathbf{u}\cdot\mathbf{u}_r-\mu_s)\rho_v''[\mathbf{u},\mathbf{u}_r,\mathbf{n}(\mathbf{u},\mathbf{r})]\mathbf{u}\cdot\mathbf{n}(\mathbf{u},\mathbf{r})\,d\Omega(\mathbf{u})\,d\Omega_r(\mathbf{u}_r)\,d\mathbf{r}}{\int_{V_F}\int_{4\pi}\int_{4\pi}\rho_v''[\mathbf{u},\mathbf{u}_r,\mathbf{n}(\mathbf{u},\mathbf{r})]\mathbf{u}\cdot\mathbf{n}(\mathbf{u},\mathbf{r})\,d\Omega(\mathbf{u})\,d\Omega_r(\mathbf{u}_r)\,d\mathbf{r}}. \tag{19}$$

$p_v(\mu_s)$ is by definition the distribution function of μ_s, which is expressed, in the local frame centered in a point I of the interface characterized by the normal $\mathbf{n}$, as

$$-\mu_s = \mu_i\mu_r + \sqrt{(1-\mu_i^2)(1-\mu_r^2)}\cos(\phi_i-\phi_r), \tag{20}$$

where

$$\mu_i = -\mathbf{n}\cdot\mathbf{u}, \quad \mu_r = \mathbf{n}\cdot\mathbf{u}_r \tag{21}$$

are the cosines associated with the incident and reflected angles, respectively, and $\pi+\phi_i$ and ϕ_r the azimuthes of the corresponding rays, respectively.

The distribution function $F(\mu_i)$ of μ_i is easily obtained in the previous Monte Carlo calculation and the reflection law is assumed known. Consequently, the phase function $p_v(\mu_s)$ is directly obtained. This approach can easily be generalized to a polarized radiation.

The previous approach is general. In the following, we only consider diffuse and specular reflection laws or their combination. In the case of a diffuse reflection law, ϕ_r and μ_r are uniformly distributed in the ranges $[0,2\pi[$ and $[0,1]$, respectively, and the spectral absorptivity $\alpha_{v\mathrm{diff}}$ depends neither on μ_i nor on ϕ_i. On the other hand, the specular reflection law is defined by

$$\mu_i = \mu_r, \quad \cos(\phi_i-\phi_r) = -1 \tag{22}$$

and we use here the approximated expression

$$\alpha'_{v\mathrm{spec}}(\mu_i) = 1-\rho'^{\mathrm{h}}_{v\mathrm{spec}}(\mu_i) = (3/2)\alpha^{\mathrm{h}}_{v\mathrm{spec}}\mu_i, \tag{23}$$

where $\rho'^{\mathrm{h}}_{v\mathrm{spec}}(\mu_i)$ is the directional-hemispherical reflectivity defined in the sense of [18] and $\alpha^{\mathrm{h}}_{v\mathrm{spec}}$ the hemispherical absorptivity given by Eq. (13).

2.4. Porous medium characterization

The practical identification of β, κ_v and σ_v requires the definition of a reference length scale which characterizes the porous medium. In practice, the transverse length scale $\mathscr{D}$ is

$$\mathscr{D} = 4/\mathscr{A}. \tag{24}$$

In the particular case of ducts, $\mathscr{D}$ is equal to the hydraulic diameter. It appears from Eq. (16) that $\mathscr{D}$ is also the extinction length β^{-1} at the optically thin limit. It is worth noticing that the choice of this length scale is pertinent as long as the solid is opaque. Indeed, radiative transfer occurs only in the fluid phase and the homogenized continuous medium introduced here is only equivalent to the fluid phase and the interface, as discussed in [19,20] and in Section 5.

As the porous medium is considered statistically isotropic and homogeneous, $\mathscr{A}$ can be easily calculated from the chord length distribution function of the fluid phase $E(s)$. A chord is defined as a segment of the fluid phase which links two interface points I and I'. From this definition, it can be easily established [21] that

$$E(s) = -(4/\mathscr{A})\,dF_e/ds, \tag{25}$$

where $F_e(s)$ is the distribution function introduced in Eq. (1). It is worthy of notice that Eq. (25) is more general than the classical relations [22–24]:

$$\mathscr{A} = 4\Big/\int_0^\infty sE(s)\,ds, \tag{26}$$

$$F_e(0) = \mathscr{A}/4. \tag{27}$$

3. Application to overlapping transparent or opaque spheres

The general method is here applied to virtual porous media, which are sets of Dispersed radius Overlapping Opaque solid Spheres (DOOS) in a transparent fluid or of Dispersed radius Overlapping Transparent fluid Spheres (DOTS) in a solid phase. The sphere centers are randomly located. Moreover, these systems allow fast calculations of I and of μ_i.

3.1. Porous medium characterization

Let us first consider a porous medium of DOOS type, characterized by a sphere center density n (in m^{-3}) and by a given radius distribution function $f_R(R)$. The porosity Π of this porous medium and the specific interface area per unit volume of the fluid phase $\mathscr{A}$ are given by [21,25,26]:

$$\begin{aligned} n^+ &= n\langle R\rangle^3 4\pi/3,\\ \Pi &= \exp[-n^+\langle R^3\rangle/\langle R\rangle^3],\\ \mathscr{A}^+ &= \mathscr{A}\langle R\rangle = 3n^+(\langle R^2\rangle/\langle R\rangle^2)\\ &= -3(\langle R^2\rangle\langle R\rangle/\langle R^3\rangle)\ln[\Pi], \end{aligned} \tag{28}$$

where $\langle\ \rangle$ stands for averaging over the sphere radius distribution. In the particular case of a set of Identical Overlapping Opaque Spheres (IOOS), i.e. DOOS model with a Dirac δ radius distribution, these expressions simplify into [24–26]

$$\begin{aligned} &n^+ = nR^3 4\pi/3, \\ &\Pi = \exp[-n^+], \\ &\mathscr{A}^+ = \mathscr{A}R = 3n^+ = -3\ln[\Pi]. \end{aligned} \tag{29}$$

Let us now consider a porous medium of DOTS type. The expressions of Π and $\mathscr{A}$ can be easily deduced from Eqs. (28):

$$\begin{aligned} &n^+ = n\langle R\rangle^3 4\pi/3, \\ &\Pi = 1 - \exp[-n^+\langle R^3\rangle/\langle R\rangle^3], \\ &\mathscr{A}^+ = \mathscr{A}\langle R\rangle \\ &\quad = 3n^+(\langle R^2\rangle/\langle R\rangle^2)/(\exp[n^+\langle R^3\rangle/\langle R\rangle^3] - 1) \\ &\quad = -3(\langle R^2\rangle\langle R\rangle/\langle R^3\rangle)\ln(1-\Pi)(\Pi^{-1} - 1). \end{aligned} \tag{30}$$

In the particular case of a set of Identical Overlapping Transparent Spheres (IOTS), i.e. DOTS model with a Dirac δ radius distribution, these expressions simplify in

$$\begin{aligned} &n^+ = nR^3 4\pi/3, \\ &\Pi = 1 - \exp[-n^+], \\ &\mathscr{A}^+ = -3\ln(1-\Pi)(\Pi^{-1} - 1) \\ &\quad = 3n^+/[\exp(n^+) - 1]. \end{aligned} \tag{31}$$

3.2. Trajectories

An important number of trajectories *MI* are generated in the Monte Carlo method in order to obtain G_e, G_a and $F_i(\mu_i)$. We have typically considered, for a given virtual porous medium defined by n, Π or $\mathscr{A}$, 10^4 geometrical realizations (given sets of center locations and radii). For each geometrical realization, we have typically used 100 trajectories (defined by M and I), i.e. 10^6 trajectories for a given virtual porous medium.

In practice, the calculations of trajectories are carried out inside a cube of edge 1. All the starting points M of the trajectories are stochastically chosen in a cube of edge 0.2, centered in the previous one. Any trajectory *MI* of length less than 0.4 is then completely included in the cube of edge 1. As discussed in Section 3.3, for a given value of $\mathscr{A}$ or of the porosity Π, the considered trajectory lengths are less than s_{max}, i.e.

$$s_{max} = 3\mathscr{D} = 12/\mathscr{A} = 12\langle R\rangle/\mathscr{A}^+. \tag{32}$$

Consequently, for a given value of $\mathscr{A}$, s_{max} is taken equal to 0.4, and, for a given radius distribution function, $\langle R\rangle$ is taken equal to $\mathscr{A}^+/30$. Typically 100–20,000 overlapping spheres are considered, depending on $\mathscr{A}$ or Π values, for a given geometrical realization.

3.3. Practical β and κ_v identification

The practical β and κ_v identification is here detailed for DOOS or DOTS morphology models and diffuse or specular reflection law. The case of the combination of these laws will be discussed in Section 5. When considering the diffuse reflection law, only β has to be identified. In this case, Eq. (11) links κ_{vdiff} to β. When considering the specular reflection law, both β and κ_{vspec} have to be identified.

For DOOS model, the chord distribution in the fluid phase is rigorously exponential [21], which is an ideal case:

$$\begin{aligned} E(s) &= -(3/4)(\langle R^2\rangle/\langle R^3\rangle)\ln[\Pi]\Pi^{[(3/4)(\langle R^2\rangle/\langle R^3\rangle)s]} \\ &= (\mathscr{A}/4)\exp[-(\mathscr{A}/4)s]. \end{aligned} \tag{33}$$

As a consequence, $1 - G_e$ is actually exponential and G_e can be rigorously identified to g_e, which leads to

$$\beta = \mathscr{A}/4, \tag{34}$$

a result identical to that obtained at the optically thin limit. Moreover, the μ_i distribution function $F_i(\mu_i)$ is linear:

$$F_i(\mu_i) = 2\mu_i, \tag{35}$$

a result which can be proved as follows. Let us consider a cylindrical frame of center M and axis $\mathbf{u}$ and statistical realizations of DOOS media (characterized by sets of centers $C_j(r_j, z_j, \theta_j)$ and radii R_j) for which M lays in the fluid phase. $F_i(\mu_i)\,d\mu_i$ is the probability over the statistical realizations that $\mu_i \leqslant -\mathbf{n}\cdot\mathbf{u} \leqslant \mu_i + d\mu_i$. In a given realization, the ray $(M, \mathbf{u})$ hits the sphere k of center C_k characterized by the non-dimensional radial coordinate $r_k^+ = r_k/R_k$. As, on one hand, the random variable $r_k^{+^2}$ is uniformly distributed in the range $[0, 1]$ and, on the other hand,

$$(\mathbf{n_k}\cdot\mathbf{u})^2 = 1 - r_k^{+^2}, \tag{36}$$

μ_i^2 is uniformly distributed in the range $[0, 1]$, independently of the distance MI and $F_i(\mu_i)$ is linear, given by Eq. (35) and is statistically independent of the other parameters characterizing a current ray. As a benchmark case, this result has also been obtained by the Monte Carlo simulation with a relative standard deviation less than 10^{-6}.

In these conditions, the specular reflection law leads from Eqs. (9), (13) and (35) to

$$F_a(s) = F_e(s)\int_0^1 \alpha'_{vspec}(\mu_i)F_i(\mu_i)\,d\mu_i = F_e(s)\alpha^h_{vspec} \tag{37}$$

and

$$\kappa_{vspec} = (\mathscr{A}/4)\alpha^h_{vspec} = \beta\alpha^h_{vspec}. \tag{38}$$

In conclusion, in the case of the DOOS model, κ_v is rigorously identified, as β has been, and is equal to the result at the optically thin limit.

On the contrary, for DOTS models the chord distribution function is not exponential. An optimal value of

$$\beta^+ = \beta\mathscr{D} = 4\beta/\mathscr{A} \tag{39}$$

is identified by minimizing the following relative error function:

$$\mathscr{E}_e(\beta^+) = \left\{ \sum_{i=0}^{N} [G_e(s_i^+) - g_e(s_i^+)]^2 \Big/ \sum_{i=0}^{N} [1 - G_e(s_i^+)]^2 \right\}^{1/2}, \tag{40}$$

where $s_i^+ = s_i/\mathscr{D}$ are the calculation discretized lengths, chosen in the range $[0,3]$ in order to cover the whole practical range of optical thickness (defined from the asymptotic value of β at the optically thin limit). In practice, the actual optical thickness is larger than this estimated value (i.e. $\beta^+ \geqslant 1$) and the actually considered optical thickness range is wider than $[0,3]$. Typically, N is chosen equal to 200. It has been established that a better spatial discretization ($N = 400$) leads to a typical relative variation of the optimal β value less than 5×10^{-5}. On the contrary, the discretization $N = 100$ leads to a typical relative variation of the optimal β value of about 10^{-2}. No significant variation of $\mathscr{E}_e$ is observed with a discretization better than $N = 200$.

An example of β^+ identification is illustrated in Fig. 3 in the particular case of IOTS model (fixed radii). The extinction cumulated distribution function G_e is compared: (i) with its adjustment; (ii) with the optically thin limit result

$$G_e = 1 - \exp[-s^+]. \tag{41}$$

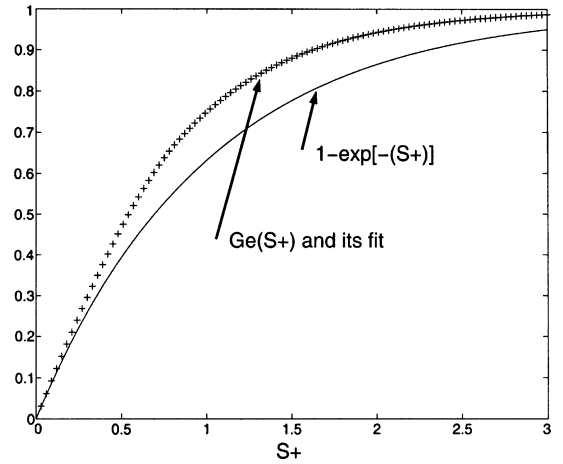

Fig. 3. β identification: (++) $G_e(s^+)$ for IOTS medium with $\mathscr{A}^+ = 1.698$.

For a specular reflection law, a non-dimensional absorption coefficient κ^+, defined by

$$\kappa^+ = \kappa_{vspec}/(\beta\alpha^h_{vspec}), \tag{42}$$

where β is the previously determined value, is also introduced in the case of the DOTS model.

As β has been previously determined, κ^+ can be obtained by identifying $G^*_a(s)$, calculated by the Monte Carlo method, i.e.

$$G^*_a(s) = \int_s^\infty F_a(s')\,ds', \tag{43}$$

with the corresponding function in the continuous medium approach, i.e.

$$\int_s^\infty f_a(s')\,ds' = \exp(-\beta s)\kappa_{vspec}/\beta, \tag{44}$$

which is equivalent to the identification of Eqs. (6) and (7). In this case also, s_i^+ is taken in the range $[0,3]$.

In practice, the relative error function

$$\mathscr{E}_a(\kappa^+) = \left\{ \sum_{i=0}^{N} \{G^*_a(s_i^+) - \alpha^h_{vspec}\kappa^+ \exp[-\beta^+ s_i^+]\}^2 \Big/ \sum_{i=0}^{N} [G^*_a(s_i^+)]^2 \right\}^{1/2} \tag{45}$$

is minimized. As in the case of the fit of β^+, N is chosen equal to 200.

Optimal values of β^+ and the associated least square fit relative errors $\mathscr{E}_e(\beta^+)$ are plotted versus $\mathscr{A}^+$ and Π in Figs. 4 and 5, respectively, for DOTS model and three different radius distributions: (i) Dirac distribution (IOTS model); (ii) Gauss distribution. The radii are then

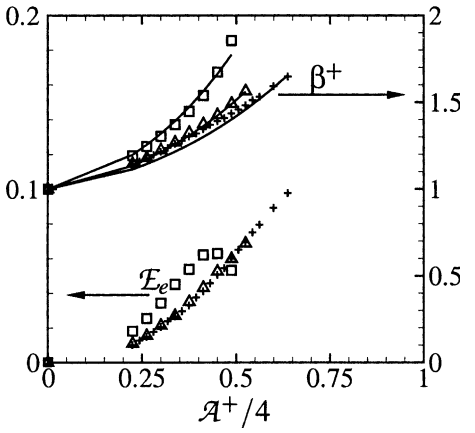

Fig. 4. Identified values of β^+ and corresponding relative error $\mathscr{E}_e$: (+) IOTS model; (△) DOTS model with a Gaussian radius distribution; (□) DOTS model with an uniform radius distribution; (—) Eq. (46).

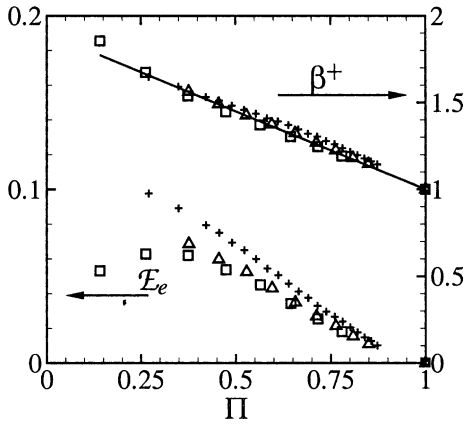

Fig. 5. Identified values of β^+ and corresponding relative error $\mathscr{E}_e$: (+) IOTS model; (△) DOTS model with a Gaussian radius distribution; (□) DOTS model with an uniform radius distribution; (—) Eq. (46).

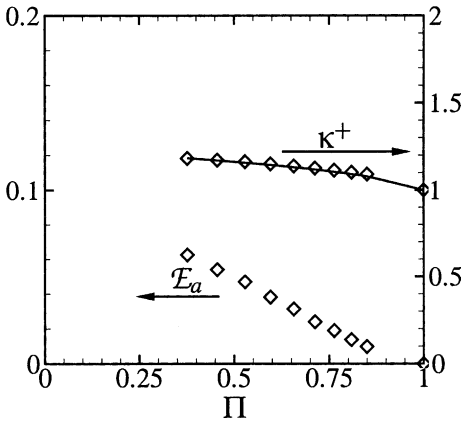

Fig. 7. Identified values of κ^+ and corresponding relative error $\mathscr{E}_a$: (◇) DOTS model with a Gaussian radius distribution; (—) Eq. (47).

given by $\langle R\rangle \min[\max(1+0.25z, 0.01), 1.99]$ in which z is a Gaussian random variable, such as $\langle z\rangle = 0$ and $\langle z^2\rangle = 1$; (iii) uniform distribution. The radii are then given by $\langle R\rangle[1 + 0.9 \times (2y - 1)]$ in which y is a uniform random variable in $[0, 1]$.

In case (ii) with a specular reflection law, optimal values of κ^+ and the associated least square fit relative errors $\mathscr{E}_a(\kappa^+)$ are plotted versus $\mathscr{A}^+$ and Π in Figs. 6 and 7, respectively.

For expressing β^+ in the three cases (i)–(iii), the porosity Π is a more pertinent parameter than the non-dimensional specific area per unit fluid volume $\mathscr{A}^+$. Indeed, the radius distribution slightly modifies the relation between β^+ and Π, which has been adjusted by a linear function with a 0.023 least square relative standard deviation, i.e.

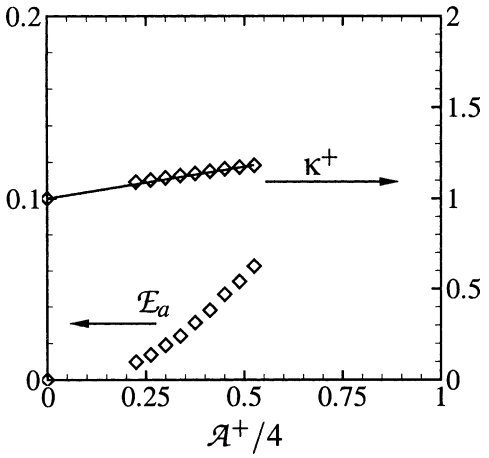

Fig. 6. Identified values of κ^+ and corresponding relative error $\mathscr{E}_a$: (◇) DOTS model with a Gaussian radius distribution; (—) Eq. (47).

$$\beta^+ \approx 1 + 0.90(1 - \Pi). \tag{46}$$

As discussed before, β^+ is equal to 1 at the optically thin limit ($\Pi \approx 1$ or $\mathscr{A}^+ \approx 0$). It is worth of notice that the least square fit error $\mathscr{E}_e(\beta^+)$ increases when the porosity decreases. A criterion of validity of the extinction homogenization hypothesis can be deduced: for a given maximum relative error $\mathscr{E}_e(\beta^+) = 0.05$, the homogenization is valid for Π in the range $[0.625, 1]$, in the case of the studied DOTS media.

It has already been shown that κ^+ is equal to unity for a diffuse reflection law. For expressing κ^+, the non-dimensional specific area per unit fluid volume $\mathscr{A}^+$ is, on the contrary of β^+ case, the most pertinent parameter. Indeed, for the specular reflection law given by Eqs. (22) and (23), κ^+ has been adjusted, in the most common case of a DOTS model with a Gaussian radius distribution, by a linear function vs. $\mathscr{A}^+$ with a 0.006 least square relative error, as shown in Fig. 6, i.e.

$$\kappa^+ \approx 1 + 0.35(\mathscr{A}^+/4). \tag{47}$$

Results very closed of Eq. (47) have been obtained for a IOTS model and a DOTS model with an uniform radius distribution. The least square fit error $\mathscr{E}_a(\kappa^+)$ increases as $\mathscr{A}^+$ increases and is lower than the corresponding error for extinction. As a consequence, the validity range obtained for extinction is also valid for absorption.

4. Phase function identification

In this section, the expressions of the phase function $p_v(\mu_s)$ are calculated analytically or from the Monte Carlo method from $F_i(\mu_i)$ and are discussed, both in the cases of DOOS or DOTS models, with a diffuse or a specular reflection law. Let us recall that $p_v(\mu_s)$ is the

distribution function of the scattering cosine μ_s which is defined by Eq. (18) and can be expressed by Eq. (20) from the μ_i distribution function $F_i(\mu_i)$ and the reflexion law.

In the case of the DOOS model, the μ_i distribution function $F_i(\mu_i)$ is given by Eq. (35). The specular reflection law modeled by Eqs. (22) and (23) leads to the following analytical results:

$$\mu_s = 1 - 2\mu_i^2,$$
$$p_{v\text{spec}}(\mu_s) = [1 - (3/2)\alpha^h_{v\text{spec}}\sqrt{(1-\mu_s)/2}]/[2(1-\alpha^h_{v\text{spec}})]. \tag{48}$$

For a diffuse reflection law, $p_{v\text{diff}}(\mu_s)$ is numerically calculated from Eq. (20) by a Monte Carlo method. The Monte Carlo result is plotted in Fig. 8 and has been adjusted by the linear function

$$p_{v\text{diff}}(\mu_s) = (1-\mu_s)/2, \tag{49}$$

with an excellent 8×10^{-5} relative least square fit standard deviation. This simple expression has to be established, to our knowledge.

In the case of a DOTS model, the distribution function $F_i(\mu_i)$ is obtained from the Monte Carlo simulations as explained in Section 2. The specular reflection law, modeled by Eqs. (22) and (23), leads to

$$\mu_s = 1 - 2\mu_i^2,$$
$$p_{v\text{spec}}(\mu_s)\,d\mu_s = \frac{F_i(\mu_i)\rho'_{v\text{spec}}(\mu_i)\,d\mu_i}{\int_0^1 F_i(\mu_i)\rho'_{v\text{spec}}(\mu_i)\,d\mu_i} = \frac{F_i[\sqrt{(1-\mu_s)/2}]\rho'_{v\text{spec}}[\sqrt{(1-\mu_s)/2}]}{[4\sqrt{(1-\mu_s)/2}\int_0^1 F_i(y)\rho'_{v\text{spec}}(y)\,dy]}\,d\mu_s. \tag{50}$$

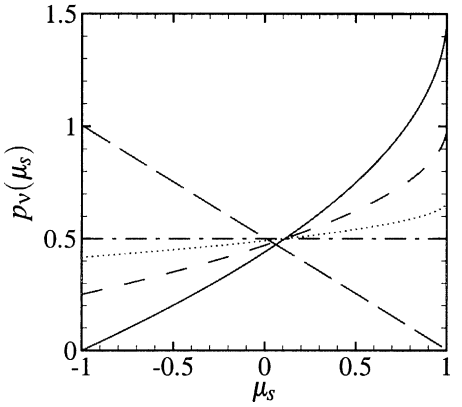

Fig. 8. Identified phase functions obtained from a DOOS model. Diffuse reflection (long-dashed). Specular reflection: $\rho_v^h = 0.33$ (solid); $\rho_v^h = 0.5$ (dashed); $\rho_v^h = 0.75$ (dotted); $\rho_v^h = 1$ (dash-dotted).

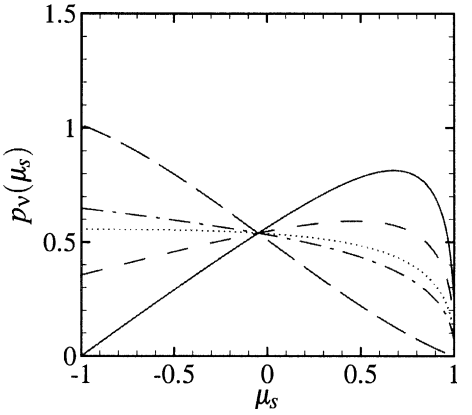

Fig. 9. Identified phase functions obtained from a IOTS model. Diffuse reflection (long-dashed). Specular reflection: $\rho_v^h = 0.33$ (solid); $\rho_v^h = 0.5$ (dashed); $\rho_v^h = 0.75$ (dotted); $\rho_v^h = 1$ (dash-dotted).

For a diffuse reflection law, $p_{v\text{diff}}(\mu_s)$ is also calculated numerically from Eq. (20) by a Monte Carlo method.

Examples of identified phase functions are plotted in Figs. 8 and 9 for DOOS and IOTS models, respectively. When considering a diffuse reflection law, forward scattering is weak in as much as it requires both incident and scattered grazing rays. On the contrary, back scattering is then very strong. On the other hand, when considering the specular reflection law with directional reflectivity given by Eq. (23), grazing rays are more reflected than other rays; consequently, forward scattering is strong and back scattering weak, as shown in Figs. 8 and 9. This effect decreases as ρ_v^h increases up to 1. Indeed, at this limit, there is no more difference between grazing rays and normal reflecting rays.

As shown in Fig. 9, the phase functions obtained in the case of a IOTS model with a specular reflection law are not monotonic. This behavior is explained by the competition between two effects: (i) grazing rays are more reflected than other rays; (ii) the concavity of the local structure drastically reduces the weight of the grazing rays and, consequently, the forward scattering.

5. Practical implementation of data

The previous results can be generalized to the case of a linear combination of diffuse and specular reflection laws at the interface. Let us notice that the extinction coefficient β of the equivalent medium is independent of the reflection law for a given porous morphology. The directional-hemispherical reflectivity $\rho'^h_v(\mu_i)$ is written

$$\rho'^h_v(\mu_i) = k\rho'^h_{v\text{spec}}(\mu_i) + (1-k)\rho_{v\text{diff}}, \quad 0 \leqslant k \leqslant 1, \tag{51}$$

where $\rho'^{h}_{v\text{spec}}$ is given by Eq. (23) and $\rho_{v\text{diff}} = 1 - \alpha_{v\text{diff}}$. The directional absorptivity of such an interface is then (see for instance [27])

$$\alpha'_v(\mu_i) = k\alpha'_{v\text{spec}}(\mu_i) + (1-k)\alpha_{v\text{diff}}. \quad (52)$$

Pure specular and diffuse absorption coefficients $\kappa_{v\text{spec}}$ and $\kappa_{v\text{diff}}$, associated with $\alpha'_{v\text{spec}}(\mu_i)$ and $\alpha_{v\text{diff}}$, respectively, have been defined as

$$\kappa_{v\text{spec}} = (\mathscr{A}\beta^+/4)\kappa^+\alpha^h_{v\text{spec}}, \quad \kappa_{v\text{diff}} = (\mathscr{A}\beta^+/4)\alpha^h_{v\text{diff}}, \quad (53)$$

where $\alpha^h_{v\text{spec}}$ is the specular hemispherical absorptivity; κ^+ is defined by Eq. (42) and β^+ by Eq. (39). As the actual contributions of photons, the diffuse and specular contributions are additive. The equivalent medium absorption coefficient is then

$$\kappa_v = k\kappa_{v\text{spec}} + (1-k)\kappa_{v\text{diff}}. \quad (54)$$

Pure specular and diffuse scattering coefficients $\sigma_{v\text{spec}}$ and $\sigma_{v\text{diff}}$ are also defined by

$$\begin{aligned}\sigma_{v\text{spec}} &= (\mathscr{A}\beta^+/4)(1-\kappa^+\alpha^h_{v\text{spec}}),\\ \sigma_{v\text{diff}} &= (\mathscr{A}\beta^+/4)(1-\alpha_{v\text{diff}}).\end{aligned} \quad (55)$$

The equivalent medium scattering coefficient is then

$$\sigma_v = k\sigma_{v\text{spec}} + (1-k)\sigma_{v\text{diff}}, \quad (56)$$

obviously equal to $\beta - \kappa_v$.

The phase function $p_v(\mu_s)$ is also a linear combination of $p_{v\text{spec}}(\mu_s)$ and $p_{v\text{diff}}(\mu_s)$, the pure specular and diffuse phase functions defined in Section 4, respectively, i.e.

$$p_v(\mu_s) = (k\sigma_{v\text{spec}}/\sigma_v)p_{v\text{spec}}(\mu_s) + [(1-k)\sigma_{v\text{diff}}/\sigma_v]p_{v\text{diff}}(\mu_s). \quad (57)$$

The radiative transfer equation has to be applied, with the previously identified coefficients κ_v and σ_v and phase function p_v, and averaged on a volume element dV_F of the fluid phase included in the current element dV of the porous medium. Let us notice, I'_{vF} the corresponding averaged local directional intensity. In practice, we consider in the continuous medium approach, for which the separation between solid and fluid phases vanishes, an equivalent averaged local directional intensity I'_v, defined by

$$I'_v\,dV\,d\Omega\,dv = I'_{vF}\,dV_F\,d\Omega\,dv, \quad (58)$$

i.e. $I'_v = \Pi I'_{vF}$. Consequently, as in [20], the radiative power per unit volume P^R in use in the continuous medium approach is equal to

$$P^R = \Pi P^R_F, \quad (59)$$

where P^R_F is calculated from the identified data. Briefly summarized, the radiative transfer equation is used with the identified data and Π is introduced in the expression of P^R. Boundaries conditions have to be written, as in [20], by taking separately account of the solid boundary surface, opaque in the present case, and of the fluid boundary surface characterized by I'_{vF}.

6. Conclusion

A general model for directly characterizing the radiative properties of porous media, which can be from the radiative point of view represented by a continuous medium, has been developed by using a Monte Carlo technique. Two original features of this method are: (i) to be independent of any radiative transfer model; (ii) to lead directly to the scattering phase function.

The model has been applied to both sets of DOOS in a transparent fluid and sets of DOTS in an opaque solid. In this model, the solid phase is assumed opaque, the fluid phase transparent and diffraction effects negligeable. An identification process of radiative data could be divided into three steps: (i) experimental determination and numerization of the morphology of slabs of an actual material; (ii) Monte Carlo calculations, defined in the present paper, either on the actual numerized data or by using an equivalent DOOS or DOTS model for the material; (iii) experimental validation from comparisons of predicted directional reflectivity and transmissivity of porous slabs and direct corresponding measurements on samples used in the morphology determination. The interest of this approach is to replace an usual inverse method scheme by only direct approaches.

Acknowledgements

M. Tancrez acknowledges the financial support of ADEME and Gaz de France for his work of "Thèse de Doctorat".

References

[1] J.R. Howell, M.J. Hall, J.L. Ellzey, Combustion of hydrocarbon fuels within porous inert media, Prog. Energy Combust. Sci. 22 (1996) 121–145.
[2] D. Baillis, J.F. Sacadura, Thermal radiation properties of dispersed media: theoretical prediction and experimental characterization, J. Quant. Spectrosc. Radiat. Transfer 67 (2000) 327–363.
[3] P.F. Hsu, J.R. Howell, Measurements of thermal conductivity and optical properties of porous partially stabilized zirconia, Exp. Heat Transfer 5 (1993) 293–313.
[4] D. Doermann, J.F. Sacadura, Heat transfer in open cell foam insulation, J. Heat Transfer 118 (1996) 88–93.
[5] D. Doermann, Modélisation des transferts thermiques dans les matériaux semi-transparents de type mousse à pores ouverts et prédiction des propriétés radiatives, Thèse de doctorat, INSA Lyon, France, 1995.

[6] D. Baillis, M. Raynaud, J.F. Sacadura, Spectral radiative properties of open cell foam insulation, J. Thermophys. Heat Transfer 13 (1999) 292–298.
[7] T.J. Hendricks, J.R. Howell, Absorption/scattering coefficients and scattering phase function in reticulated porous ceramics, J. Heat Transfer 118 (1) (1996).
[8] T.J. Hendricks, J.R. Howell, Inverse radiative analysis to determine spectral radiative properties using the discrete ordinates method, in: International Heat Transfer Conference, Brighton, 1994.
[9] D. Baillis, J.F. Sacadura, Identification of polyurethane foam radiative properties-influence of transmittance measurements number, J. Thermophys. Heat Transfer (2002) 200–212.
[10] Y.S. Yang, J.R. Howell, D.E. Klein, Radiative heat transfer through a randomly packed bed of spheres by the Monte Carlo method, J. Heat Transfer 105 (1983) 325.
[11] C. Argento, D. Bouvard, A ray tracing method for evaluating the radiative heat transfer in porous media, Int. J. Heat Mass Transfer 39 (15) (1996) 3175–3180.
[12] K. Kudo, Y.M. Taniguchi, Y.M. Kim, W.J. Yang, Transmittance of radiative energy through three-dimensional packe spheres, ASME/JSME Thermal Eng. Proc. 4 (1991) 35–42.
[13] O. Rozenbaum, D. De Sousa Meneses, P. Echegut, P. Levitz, Influence of the texture on the radiative properties of semitransparent materials. Comparison between model and experiment, High Temp. High Pressure 32 (1) (2000) 61–66.
[14] M.P. Mengüc, Shanker Subramaniam, Solution of the inverse radiation problem for inhomogeneous and anisotropically scattering media using a Monte Carlo technique, Int. J. Heat Mass Transfer 34 (1) (1991) 253–266.
[15] B.P. Singh, M. Kaviany, Independant theory versus direct simulation of radiation heat transfer in packed beds, Int. J. Heat Mass Transfer 34 (11) (1991) 2869–2882.
[16] B.P. Singh, M. Kaviany, Modelling radiative heat transfer in packed beds, Int. J. Heat Mass Transfer 35 (6) (1992) 1397–1405.
[17] B.P. Singh, M. Kaviany, Effects of solid conductivity on radiative heat transfer in packed beds, Int. J. Heat Mass Transfer 37 (16) (1994) 2579–2583.
[18] R. Siegel, J.R. Howell, Thermal Radiation Heat Transfer, third ed., Taylor and Francis, 1992.
[19] M. Tancrez, M. Hilka, J. Taine, Comparison between local and homogenized models of radiative transfer in a set of parallel ducts considered as a porous medium, Int. J. Heat Mass Transfer 45 (2002) 173–180.
[20] M. Tancrez, J. Taine, Radiative behavior of a honeycomb radiant burner, in: Proceedings of The Third International Symposium on Radiative Transfer, ICHMT, June 2001.
[21] S. Torquato, B. Lu, Chord-length distribution for two-phase random media, Phys. Rev. E 47 (4) (1993).
[22] O. Rozenbaum, Etude de l'influence de la texture sur l'émissivité spectrale de matériaux poreux semi-transparents à haute température, Thèse de doctorat, Université d'Orléans, 1999.
[23] P. Levitz, Off latice reconstruction of porous media: critical evaluation, geometrical confinement and molecular transport, Adv. Colloid Interface Sci. (1998) 71–106.
[24] A.P. Roberts, Statistical reconstruction of three-dimensional porous media from two-dimensional images, Phys. Rev. 56 (1997) 3203–3212.
[25] H.L. Weissberg, Effective diffusion coefficient in porous media, J. Appl. Phys. 34 (9) (1963) 2636–2639.
[26] H.L. Weissberg, S. Prager, Viscous flow through porous media. II. Approximate three point correlation function, Phys. Fluids 5 (11) (1962) 1390–1392.
[27] R. Carminati, J.-J. Greffet, A. Sentenac, A model for the radiative properties of opaque rough surfaces, in: The Eleventh International Heat Transfer Conference, Kyongju, South Korea, August 1998, vol. 7, pp. 427–432.